Spin-half Heisenberg antiferromagnet on two archimedian lattices: From the bounce lattice to the maple-leaf lattice and beyond

D. J. J. Farnell,[1] R. Darradi,[2] R. Schmidt,[3] and J. Richter[3]

[1]*Division of Mathematics and Statistics, Faculty of Advanced Technology, University of Glamorgan, Pontypridd, CF37 1DL, Wales, United Kingdom*

[2]*Institut für Theoretische Physik, Technische Universität Braunschweig, DE-38106 Braunschweig, Germany*

[3]*Institut für Theoretische Physik, Otto-von-Guericke Universität Magdeburg, DE-39016 Magdeburg, Germany*

(Received 12 April 2011; revised manuscript received 9 August 2011; published 2 September 2011)

We investigate the ground state of the two-dimensional Heisenberg antiferromagnet on two Archimedean lattices, namely, the maple-leaf and bounce lattices as well as a generalized J-J' model interpolating between both systems by varying J'/J from $J'/J = 0$ (bounce limit) to $J'/J = 1$ (maple-leaf limit) and beyond. We use the coupled cluster method to high orders of approximation and also exact diagonalization of finite-sized lattices to discuss the ground-state magnetic long-range order based on data for the ground-state energy, the magnetic order parameter, the spin-spin correlation functions as well as the pitch angle between neighboring spins. Our results indicate that the "pure" bounce ($J'/J = 0$) and maple-leaf ($J'/J = 1$) Heisenberg antiferromagnets are magnetically ordered, however, with a sublattice magnetization drastically reduced by frustration and quantum fluctuations. We found that magnetic long-range order is present in a wide parameter range $0 \leqslant J'/J \lesssim J'_c/J$ and that the magnetic order parameter varies only weakly with J'/J. At $J'_c \approx 1.45J$, a transition to a quantum orthogonal-dimer singlet ground state without magnetic long-range order takes place that is probably of first-order type, although we cannot rule out that this transition is second order. The orthogonal-dimer state is the exact ground state in this large-J' regime, and so our model has similarities to the Shastry-Sutherland model. Finally, we use the exact diagonalization to investigate the magnetization curve. We find a $1/3$ magnetization plateau for $J'/J \gtrsim 1.07$ and another one at $2/3$ of saturation emerging only at large $J'/J \gtrsim 3$.

DOI: 10.1103/PhysRevB.84.104406 PACS number(s): 75.10.Jm, 75.40.−s, 75.50.Ee, 75.60.Ej

I. INTRODUCTION

The study of two-dimensional (2D) quantum spin-half antiferromagnetism is an interesting and challenging problem, in particular, if the magnetic interactions are frustrated.[1,2] In 2D systems, the interplay between geometry and quantum fluctuations may lead to semi-classical ground-state (GS) phases with conventional magnetic long-range order (LRO) as well as to new quantum phases without magnetic LRO.[3,4] The spin-$\frac{1}{2}$ Heisenberg antiferromagnet (HAF) on the eleven 2D Archimedian and related lattices presents an excellent opportunity to investigate the subtle balance of interactions and fluctuations and the role of lattice geometry.[4] Archimedian lattices are uniform tilings, and so the distance between nearest-neighboring sites may be set to one. It is well established that magnetic LRO is present in the GS of the spin-$\frac{1}{2}$ HAF on bipartite lattices (square,[1,4] honeycomb,[4–6] 1/5-depleted square (or CaVO),[4,7,8] and square-hexagonal-dodecagonal[4,9]). However, this magnetic order can be weakened or even suppressed by the presence of frustration. The first investigation of a frustrated quantum HAF goes back to the early 1970s, when Anderson and Fazekas[10,11] considered the spin-$\frac{1}{2}$ HAF on the triangular lattice. They conjectured a magnetically disordered GS. However, it is now clear that there is magnetic GS LRO in this system, see, e.g., Refs. 4 and 12–16. The pioneering work of Anderson and Fazekas has formed the starting point for an intensive investigation of frustrated quantum magnetism. In particular, it has stimulated the search for nonmagnetic quantum states in 2D magnetic systems.

Another well investigated frustrated 2D system is the HAF on the SrCuBO lattice, which can be transformed by an appropriate distortion to the Shastry-Sutherland square lattice model[17] with equal strength of all exchange bonds. Again, the GS is magnetically long-range ordered, see, e.g., Refs. 18–22. However, the magnetic LRO may be destroyed by a modification of bond strengths.[17–22]

The coordination number z is quite large for the triangular ($z = 6$) and SrCuBO ($z = 5$) lattices, and that might be responsible for the semiclassical GS LRO found for the HAF on these frustrated Archimedian lattices. Thus a "nonmagnetic" quantum GS might be favored for lattices with lower coordination number z. Indeed, a regular depletion of the triangular lattice by a factor of $1/4$ yields the Archimedian kagome lattice with coordination number $z = 4$. Contrary to the triangular lattice, the GS of the spin-$\frac{1}{2}$ HAF on the kagome lattice is most likely nonmagnetic, see, e.g., Refs. 4 and 23–27. Another frustrated model with low coordination number $z = 3$ having a nonmagnetic quantum GS is the HAF on the Archimedian star lattice.[4,28–30] Moreover, we mention that the HAF on the (non-Archimedian) square-kagome lattice with $z = 4$ has most likely also a nonmagnetic quantum GS.[31–34] The above-mentioned depletion of the triangular lattice by a quarter is clearly not the only possibility. As has been pointed out by D. Betts,[35] a regular depletion of the triangular lattice by a factor of $1/7$ yields another translationally invariant lattice, namely, the Archimedian maple-leaf lattice.[4,36] The coordination number of this lattice is $z = 5$ and lies between those of the triangular ($z = 6$) and the kagome ($z = 4$) lattices. Moreover, there is a frustrated Archimedian lattice with $z = 4$, the so-called bounce lattice.[4] Both the maple-leaf and the bounce lattices might be candidates for nonmagnetic GSs. However, there are indications from previous studies (based on

 ©2011 American Physical Society

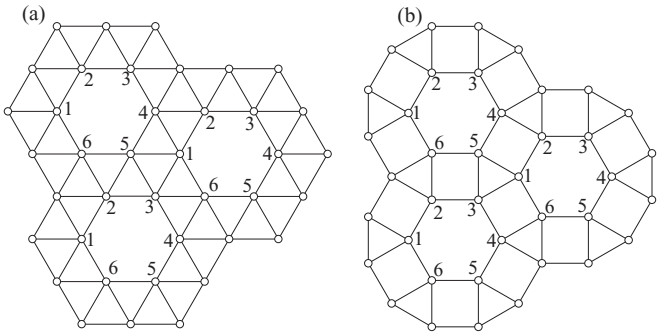

FIG. 1. Archimedian lattices: (a) 1/7-depleted triangular (maple-leaf) lattice and (b) bounce lattice. The six equivalent sublattices for both lattices are indicated by 1, 2, 3, 4, 5, and 6.

exact diagonalizations of finite-sized lattices) of semiclassical GS magnetic LRO[4,36] in the spin-$\frac{1}{2}$ HAF on these lattices. This conclusion was drawn based on only two finite lattices of $N = 18$ and $N = 36$ sites and therefore the conviction in the conclusions is lessened.

It is interesting to point out that the discussion of the magnetic properties of the HAF on Archimedian lattices is not only a challenging theoretical problem of quantum many-body physics but that it is also strongly relevant to experiment. Indeed, most of these lattices are found to be underlying lattice structures of the magnetic ions of various magnetic compounds, such as CaV_4O_9,[37] $SrCu_2(BO_3)_2$,[38] or $[Fe_3(\mu_3\text{-}O)(\mu T\text{-}OAc)_6\text{-}(H_2O)_3][Fe_3(\mu_3\text{-}O)(\mu\text{-}OAc)_{7.5}]_2{\cdot}7\ H_2O$.[39] Recently, the magnetic compound $M_x[Fe(O_2CCH_2)_2NCH_2PO_3]_6 \cdot nH_2O$ (see Ref. 40) with maple-leaf lattice structure as well as hybrid cobalt hydroxide materials[41] with maple-leaf-like lattice structure have been synthesized, which may stimulate increasing interest in this lattice. Moreover, in the natural mineral spangolite $[Cu_6Al(SO_4)(OH)_{12}Cl{\cdot}3H_20]$, the magnetic copper ions sit on the lattice sites of the maple-leaf lattice.[42,43] In particular, spangolite is a very interesting magnetic system, since magnetic copper ions carry spin 1/2 and the experimental data indicate that strong fluctuations at low temperatures are present that may prevent magnetic ordering.[43] In Ref. 43, Fennell *et al.*

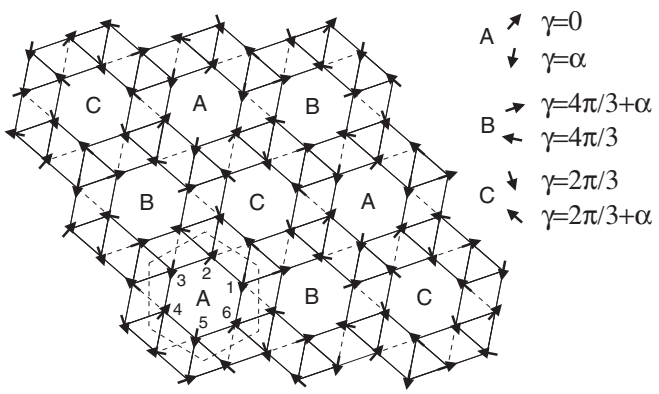

FIG. 2. Illustration of the classical GS of $J - J'$ model [Eq. (1); J represented by solid lines and J' by dashed lines]. The numbers 1, 2, 3, 4, 5, and 6 denote the six sites in the geometrical unit cell. The magnetic unit cell contains three geometrical unit cells A, B, and C.

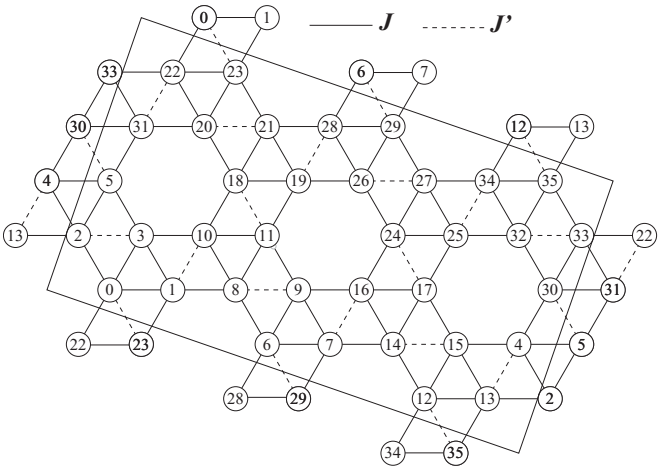

FIG. 3. The finite maple-leaf lattice of 36 sites imposing periodic boundary conditions used for the ED calculations. Removing the dashed J' bonds the the exchange pattern corresponds to the bounce lattice of $N = 36$ sites.

propose that the spin-half Heisenberg model on the maple-leaf lattice with five different exchange integrals is the relevant model for this material.

In this paper, we will discuss the GS properties of the spin-$\frac{1}{2}$ HAF on the maple-leaf and the bounce lattices, see Fig. 1. These lattices are related to each other because the bounce lattice is equivalent to a bond-depleted maple-leaf lattice, see Ref. 4 and Fig. 2. Therefore we will consider a generalized spin-$\frac{1}{2}$ J-J' HAF:

$$H = J \sum_{\langle ij \rangle} \mathbf{s}_i \cdot \mathbf{s}_j + J' \sum_{[ij]} \mathbf{s}_i \cdot \mathbf{s}_j, \quad J > 0, \quad J' \geqslant 0, \quad (1)$$

where $\langle ij \rangle$ runs over all nearest-neighbor (NN) bonds of the bounce lattice and $[ij]$ runs over all additional NN bonds present in the maple-leaf lattice, cf. Figs. 2 and 3.

A well-established method that can deal effectively with the GS properties of infinite 2D quantum magnets is given by the coupled cluster method (CCM) (see, e.g., Refs. 44–48 and references cited therein). The accuracy and effectiveness of this method in relation to the investigation of frustrated quantum spin systems has been strongly improved by the implementation of a parallelized CCM code[49] that carries out high-order CCM calculations. In particular, quantum phase transitions in 2D quantum spin systems that are driven by frustration can be studied by this method.

II. THE CLASSICAL GROUND STATE

We start with a brief illustration of the classical GS of the model (see Fig. 2), i.e., the $\mathbf{s}_i$ are treated as classical vectors of length s. The classical GSs in the limits $J' = 1$ and $J' = 0$ have already been discussed in Ref. 4. Starting from the information on the classical GS provided there it can be found easily for the $J - J'$ model. The geometrical unit cell (hexagon) contains six sites labeled by the running index $n = 1, \ldots, 6$. The magnetic unit cell is three times larger. Within one geometrical unit cell the pitch angle α between neighboring spins (e.g., the spin on sites 1 and

2) around the hexagon is given by $\alpha = \pi - \arctan(\frac{J'\sqrt{3}}{4J-J'})$. Next-nearest-neighbor spins on a hexagon (e.g., spins on sites 1 and 3) are parallel. Equivalent spins in two neighboring unit cells are rotated by a fixed angle $\pm 2\pi/3$, see the spin directions in unit cells A, B, and C shown in Fig. 2. In the limits $J' = 0$ (bounce lattice), $J' = 1$ (maple-leaf lattice), or $J' \to \infty$, one has $\alpha = \pi$ and $E = -3JNs^2/2$, $\alpha = 5\pi/6$ and $E = -(1+\sqrt{3})JNs^2/2$, or $\alpha \to \pi/3$ and $E \to -J'Ns^2/2$, respectively.

III. THE METHODS

A. Coupled cluster method

We start with a brief illustration of the main features of the coupled cluster method (CCM). For a general overview on the CCM, the interested reader is referred, e.g., to Refs. 45,47,48, and 52, and for details of the CCM computational algorithm for quantum spin systems (with spin quantum number $s = 1/2$), to Refs. 45 and 46. The starting point for a CCM calculation is the choice of a normalized model or reference state $|\Phi\rangle$, together with a set of mutually commuting multispin creation operators C_I^+, which are defined over a complete set of many-body configurations I. The operators C_I are the multispin destruction operators and are defined to be the Hermitian adjoint of the C_I^+. We choose $\{|\Phi\rangle; C_I^+\}$ in such a way that we have $\langle\Phi|C_I^+ = 0 = C_I|\Phi\rangle$, $\forall I \neq 0$. Note that the CCM formalism corresponds to the thermodynamic limit $N \to \infty$.

For spin systems, an appropriate choice for the CCM model state $|\Phi\rangle$ is often a classical spin state in which the most general situation is one in which each spin can point in an arbitrary direction. We then perform a local coordinate transformation such that all spins are aligned in the negative z direction in the new coordinate frame. As a result we have

$$|\Phi\rangle = |\downarrow\downarrow\downarrow\cdots\rangle, \quad C_I^+ = s_i^+,\ s_i^+ s_j^+,\ s_i^+ s_j^+ s_k^+, \ldots, \qquad (2)$$

(where the indices $i, j, k, \ldots$ denote arbitrary lattice sites) for the model state and the multispin creation operators, which now consist of spin-raising operators only.

The CCM parametrizations of the ket and bra ground states are given by

$$\begin{aligned} H|\Psi\rangle &= E|\Psi\rangle, \quad \langle\tilde{\Psi}|H = E\langle\tilde{\Psi}|, \\ |\Psi\rangle &= e^S|\Phi\rangle, \quad S = \sum_{I\neq 0} \mathcal{S}_I C_I^+, \\ \langle\tilde{\Psi}| &= \langle\Phi|\tilde{S}e^{-S}, \quad \tilde{S} = 1 + \sum_{I\neq 0} \tilde{\mathcal{S}}_I C_I. \end{aligned} \qquad (3)$$

The correlation operators S and $\tilde{S}$ contain the correlation coefficients $\mathcal{S}_I$ and $\tilde{\mathcal{S}}_I$ that we must determine. Using the Schrödinger equation, we note that $H|\Psi\rangle = E_g|\Psi\rangle$, and so we see from the above equations that $He^S|\Phi\rangle = E_g e^S|\Phi\rangle$. Hence, after some rearrangement and the application of $\langle\Phi|$ to both sides of this equation, we find that $E = \langle\Phi|e^{-S}He^S|\Phi\rangle$. We now need to determine the ket-state coefficients $\mathcal{S}_I$, often within some approximation. The interested reader is referred to Ref. 48 for a very detailed discussion of the CCM method and how is it applied in practice (e.g., a full LSUB2 calculation is performed explicitly and in detail). The magnetic order parameter (sublattice magnetization) is given by $M_s = -\frac{1}{N}\sum_i^N \langle\tilde{\Psi}|s_i^z|\Psi\rangle$, where s_i^z is expressed in the transformed coordinate system. (Note that all magnetic sublattices carry the same sublattice magnetization.)

To find the ket-state and bra-state correlation coefficients, we require that the expectation value $\bar{H} = \langle\tilde{\Psi}|H|\Psi\rangle$ is a minimum with respect to the bra-state and ket-state correlation coefficients, such that the CCM ket- and bra-state equations are given by

$$\langle\Phi|C_I^- e^{-S}He^S|\Phi\rangle = 0, \quad \forall I \neq 0, \qquad (4)$$

$$\langle\Phi|\tilde{\mathcal{S}}e^{-S}[H, C_I^+]e^S|\Phi\rangle = 0, \quad \forall I \neq 0. \qquad (5)$$

The problem of determining the CCM equations now becomes a pattern-matching exercise of the $\{C_I^-\}$ to the terms in $e^{-S}He^S$ in Eq. (4). Equation (4) yields N_F nonlinear coupled polynomial equations for the CCM ket-state coefficients $\mathcal{S}_I$ only [i.e., no $\tilde{\mathcal{S}}_I$ terms in Eq. (4)]. By contrast, Eq. (5) yields similarly coupled equations that are also polynomial in $\mathcal{S}_I$ but are linear only in $\tilde{\mathcal{S}}_I$.

The CCM formalism is exact if we take into account all possible multispin configurations in the correlation operators S and $\tilde{S}$. This is, however, generally not possible for quantum many-body models including that studied here. We must therefore use the most common approximation scheme to truncate the expansion of S and $\tilde{S}$ in Eqs. (4) and (5), namely, the LSUBn scheme where we include only n or fewer correlated spins in all configurations (or lattice animals in the language of graph theory), which span a range of no more than n adjacent (contiguous) lattice sites (for more details see Refs. 46 and 52). For instance, one includes multispin creation operators of one, two, three, or four spins distributed on arbitrary clusters of four contiguous lattice sites for the LSUB4 approximation. The number of these fundamental configurations can be reduced exploiting lattice symmetries. In the CCM-LSUB8 approximation, we have finally $N_F = 330\,369$ fundamental configurations.

Since the LSUBn approximation becomes exact for $n \to \infty$, it is useful to extrapolate the "raw" LSUBn data in the limit $n \to \infty$. An appropriate extrapolation rule for the order parameter of systems showing GS magnetic LRO is given by $M_s(n) = a_0 + a_1(1/n) + a_2(1/n^2)$ (see, e.g., Refs. 46 and 47) where the results of the LSUB2,4,6,8 approximations are used for the extrapolation. For the GS energy per spin, $E(n)/N = b_0 + b_1(1/n^2) + b_2(1/n^4)$ is a well-tested extrapolation ansatz.[46,47]

Although in quantum mechanics, one normally assumes that the bra state is the Hermitian conjugate of the ket state, this is not the case for the CCM. Here, one parametrizes the bra and ket states separately, although they are clearly not independent. One loses therefore the property of a variational upper bound on the ground-state energy, although in practice one often finds at a given level of approximation that the ground-state energy does indeed lie above the value for the "true" ground-state energy for the system. There are, however, a number of advantages that compensate for this loss of Hermiticity between the bra and ket states. Firstly, the Goldstone linked-cluster theorem is obeyed and so we obtain results in the infinite-lattice limit from the outset at any level of approximation. This is a strong point in favor of the method. Secondly, we do not have to resum explicitly an otherwise

infinite set of (Goldstone) diagrams. These diagrams are contained "for free" by the exponential character of the wave function, e.g., for the ket state via $e^S|\Phi\rangle$. It is crucial to note that S contains only creation operators, which allows us to do this. The exponential nature of e^S also means that the number of diagrams in the ground-state wave function are counted correctly. The basic problem inherent to the CCM now boils down to the expansion of the similarity transform $e^{-S}He^S|\Phi\rangle$, which generally terminates to finite order. As mentioned above, we then "pattern-match" C_I^- to $e^{-S}He^S|\Phi\rangle$, which is ideally suited to the computational solution to high-orders of approximation. Again, these points are also strongly in favor of the method. Finally, the important Hellmann-Feynman theorem[44] is obeyed, and so we may evaluate the properties of expectation values of any operator A (such as those results for the order parameter presented here) by using $\bar{A} = \langle\tilde{\Psi}|A|\Psi\rangle$, where $\langle\tilde{\Psi}|$ and $|\Psi\rangle$ are the usual CCM bra and ket states at a given level of approximation used also for the ground-state energy. Again, the interested reader is referred to Ref. 44 for a full exposition of the basic formalism underpinning the CCM method. However, no method is perfect and a comparison of results of the CCM to those results of the best of other approximate methods is given in Ref. 48.

B. Exact diagonalization

The Lanczos exact diagonalization (ED) is a well-established many-body method, see, e.g., Refs. 4,23,24, and 53–56. Hence, we can restrict our discussion of the method to some specific features relevant for our problem. The ED method has been successfully applied to 2D frustrated quantum spin systems, see, e.g., Refs. 4,24,54,55, and 56. Here, we follow along the lines of Ref. 4. For the system under consideration, there are only two appropriate finite lattices, namely, one with $N = 18$ (see Fig. 2 of Ref. 36) and another one with $N = 36$ (see Fig. 3). Note that these finite lattices do not have the full lattice symmetry of the infinite lattice. Moreover, the unit cell of these lattices is fairly large, namely, it contains six sites. Hence, we consider the ED data as a complementary information to confirm or to question the CCM results corresponding to the thermodynamic limit $N \to \infty$. For the finite-size order parameter, we use[4]

$$m^+ = \sqrt{\frac{(M^+)^2}{N^2}} = \left(\frac{1}{N^2}\sum_{i,j}^{N}|\langle \mathbf{s}_i \mathbf{s}_j\rangle|\right)^{1/2}. \qquad (6)$$

We extrapolate the GS energy and the order parameter as described in Ref. 4 (see also Refs. 54 and 56, and references therein). However, the results of these ED extrapolations have to be taken with caution, since they are based only on two data points.

IV. RESULTS

Henceforth, we set $J = 1$ and we consider J' as the active parameter in the model of Eq. (1). We apply high-order CCM up to LSUB8 and these infinite-lattice results are complemented by ED results of $N = 18$ and 36 sites, see Fig. 3. We choose the classical canted state illustrated in Sec. II to be the CCM reference or model state. As quantum fluctuations may lead to a "quantum" pitch angle that is different from the classical case, we consider the pitch angle α in the reference state as a free parameter. We then determine the quantum pitch angle $\alpha_{\rm qu}$ by minimizing $E_{\rm LSUB}n(\alpha)$ with respect to α in each order n.

TABLE I. CCM results for the spin-1/2 HAFM on the bounce ($J' = 0$) and on the maple-leaf ($J' = 1$) lattices. E/N is the GS energy per spin and M_s is the sublattice magnetization. The LSUBn results are extrapolated using $E(n)/N = b_0 + b_1(1/n^2) + b_2(1/n^4)$ for the GS energy and $M_s(n) = a_0 + a_1(1/n) + a_2(1/n^2)$ for the sublattice magnetization.

Bounce	E/N	M_s
LSUB2	−0.521 631	0.404 343
LSUB4	−0.546 866	0.339 357
LSUB6	−0.553 763	0.298 249
LSUB8	−0.556 998	0.265 252
Extrapolated CCM	−0.5605	0.1657
maple-leaf	E/N	M_s
LSUB2	−0.483 470	0.405 622
LSUB4	−0.512 309	0.338 483
LSUB6	−0.520 378	0.297 499
LSUB8	−0.523 861	0.265 768
Extrapolated CCM	−0.5279	0.1690

We start with the case of the perfect Archimedian bounce and maple-leaf lattices, and so we set $J' = 0$ and $J' = 1$, respectively. Results for the GS energy and sublattice magnetization are given for both lattices in Table I. GS energies agree well with the previously reported data.[4,36] Furthermore, we confirm the previous findings that the GS is magnetically ordered. However, due to quantum fluctuations and frustration, the sublattice magnetization is drastically reduced. Using our extrapolated CCM data (see Table I) we find that the sublattice magnetizations are only 33% of the classical value for the bounce lattice and 34% of the classical value for the maple-leaf lattice. However, these values are still clearly above the ED estimates (which are 22% for the maple-leaf and 27% for the bounce lattice) of Ref. 4. We believe that the CCM data reported here are more reliable than the ED estimates because these ED results were extrapolated using only two data points ($N = 18$ and 36),[50] see also Sec. III B. These rather small values of the order parameter, which are significantly below that for the triangular lattice,[4,12–16] indicate that the GS magnetic LRO is fragile, and one can speculate that slight modifications of the model parameters might lead to nonmagnetic quantum GSs. We remark again that a related experimental material called spangolite[43] did not appear to show magnetic LRO, and that this experimental result also spurs us on to evaluate the more general model.

The results for the GS energy per spin are shown in Fig. 4 as a function of J'. CCM LSUBn results for the GS energy are clearly converging rapidly with increasing n for all values of J'. We have also used our ED data for $N = 18$ and 36 to extrapolate them to $N \to \infty$ (for the details of the extrapolation, see Ref. 4). As already mentioned above, this ED extrapolation has to be taken with caution, since it is based only on two data points. We find a reasonable agreement between the CCM and ED data for the GS energy.

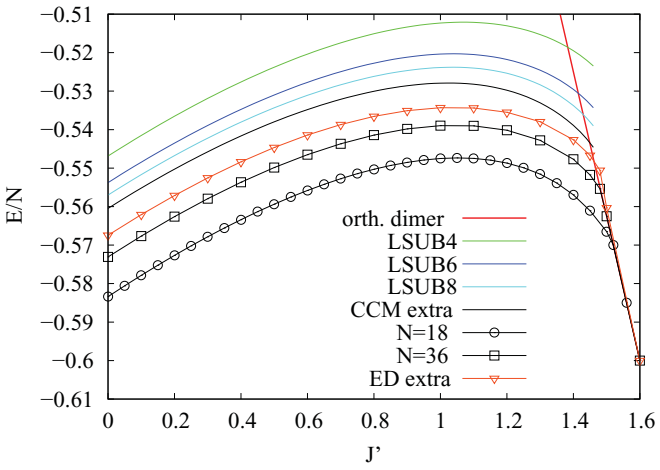

FIG. 4. (Color online) CCM results for the GS energy per spin E/N as function of J'. The CCM extrapolated values in the limit $n \to \infty$ are obtained using the extrapolation scheme $E(n)/N = b_0 + b_1(1/n)^2 + b_2(1/n)^4$. ED results for $N = 18$ and 36 as well as ED extrapolated values using the extrapolation scheme $E(N)/N = x_0 + x_1 N^{-3/2}$ are also shown. The red straight line shows the exact energy of the orthogonal-dimer state.

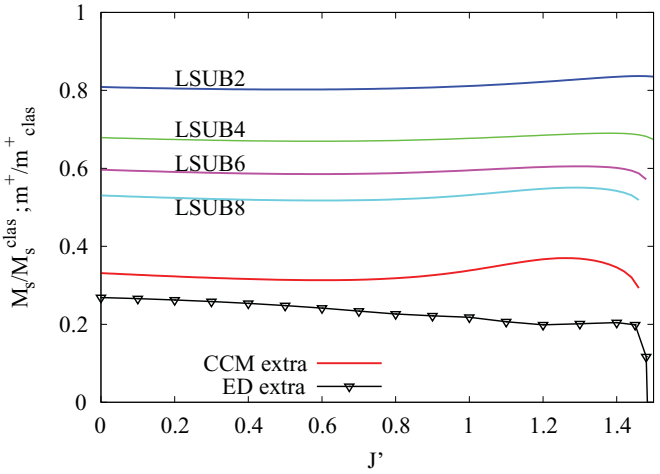

FIG. 5. (Color online) CCM results for magnetic order parameter (sublattice magnetization) M_s as function of J'. The data for the quantum model are scaled by its corresponding classical value $M_s^{\text{clas}} = 1/2$. The extrapolated values in the limit $n \to \infty$ are found using the extrapolation scheme $M_s(n) = c_0 + c_1(1/n) + c_2(1/n)^2$. We also show extrapolated finite-lattice results for the ED order parameter m^+ using the extrapolation scheme $m^+(N) = y_0 + y_1 N^{-1/2}$.

As indicated by the ED data, the GS energy becomes linear in J' at larger $J' \gtrsim 1.5$. This is related to the existence of a dimer product eigenstate where all J' bonds carry a dimer singlet.[51] We find that this singlet orthogonal-dimer eigenstate becomes the GS for $J' > J'_c$. Hence our model has much in common with the Shastry-Sutherland model[17–22] that also demonstrates a similar exact orthogonal-dimer GS. We use the intersection point between the extrapolated CCM GS energy per site and the energy of the orthogonal-dimer eigenstate given by $E_{\text{OD}}/N = -3J'/8$ to determine the transition point $J'_c = 1.449$. (Note that the corresponding value based on the ED data is $J'_c = 1.462$.)

Next we use the CCM results for the magnetic order parameter M_s to discuss the stability of magnetic LRO as a function of J', see Fig. 5. It is obvious that the magnetic LRO persists in the whole region $0 \leqslant J' \leqslant J'_c$. This conclusion is supported by the extrapolated ED order parameter also shown for comparison in Fig. 5. The obvious quantitative difference between the ED and CCM curves (which is also present in the GS energy per spin E/N, see Fig. 4) might by attributed to the limited accuracy of ED extrapolations discussed above (only two data points, the finite lattices do not have the the full lattice symmetry of the infinite lattice).

Interestingly, the dependence of the order parameter on J' is fairly weak over the whole region $0 \leqslant J' \leqslant J'_c$. Thus the extrapolated CCM order parameter varies only between 29% and 37% of its classical value $M_s^{\text{clas}} = 1/2$. This behavior might be interpreted as balanced interplay between increasing of frustration and increasing of the number of nearest neighbors when J' is growing. Our data for the order parameter lead to the conclusion that there is probably a direct first-order transition to the magnetically disordered orthogonal-dimer singlet GS, although we cannot rule out that this transition is of second-order type.

An additional confirmation of the above discussed behavior comes from the ED data for the spin-spin correlation functions $\langle \mathbf{s}_i \mathbf{s}_j \rangle$ presented in Fig. 6. Again we see that the variation of the correlation functions with J' is weak almost up to the transition point J'_c. Moreover, for $J' < J'_c$ the correlation functions of the quantum model behave similarly to those of the classical model.

Finally, in Fig. 7, we compare results for the classical pitch angle α_{cl}, see Sec. II, and for the quantum pitch angle α_{qu} calculated by the CCM. We see that both α_{cl} and α_{qu} are close to each other and that there is only a slight variation of the pitch angle with J' (the value of the quantum pitch angle in CCM-LSUB8 approximation is $\alpha_{\text{qu}} = \pi$ at $J' = 0$, $\alpha_{\text{qu}} \approx 0.895\pi$, and it is still $\alpha_{\text{qu}} \approx 0.714\pi$ at $J' = J'_c$). Moreover, the LSUB4 and LSUB8 data for α_{qu} almost coincide.

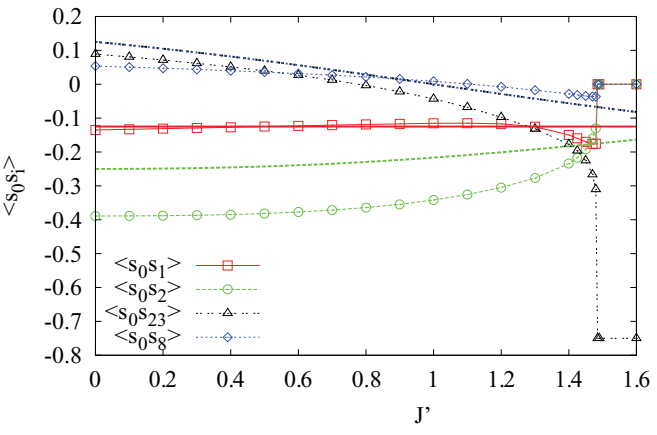

FIG. 6. (Color online) ED results for some selected spin-spin correlation functions $\langle \mathbf{s}_0 \mathbf{s}_i \rangle$, $i = 1,2,8,23$, for the finite lattice of $N = 36$ sites shown in Fig. 3. The results for the quantum $s = 1/2$ model are given by thin lines with symbols. The corresponding classical results are given by thick lines with the same color without symbols. The location of sites "0" and "i" in $\langle \mathbf{s}_0 \mathbf{s}_i \rangle$ can be found in Fig. 3. Note that the classical curves for $\langle \mathbf{s}_0 \mathbf{s}_8 \rangle$ and $\langle \mathbf{s}_0 \mathbf{s}_{23} \rangle$ coincide.

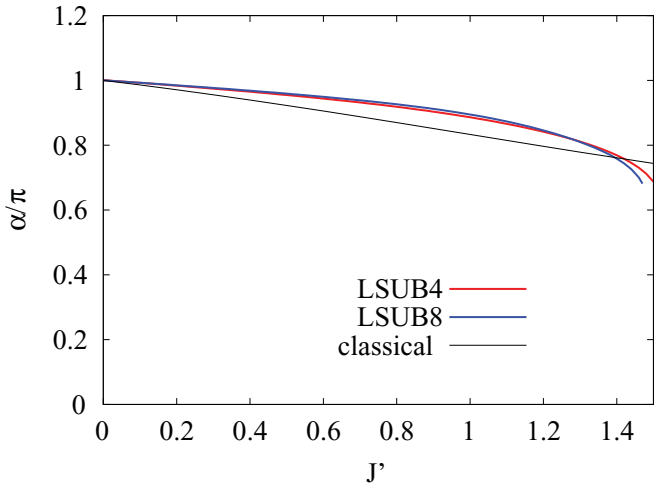

FIG. 7. (Color online) Results for the quantum pitch angle α_{qu} as a function of J' calculated within CCM-LSUBn approximation with $n = 4$ and 8. The classical result α_{cl} is shown for the sake of comparison.

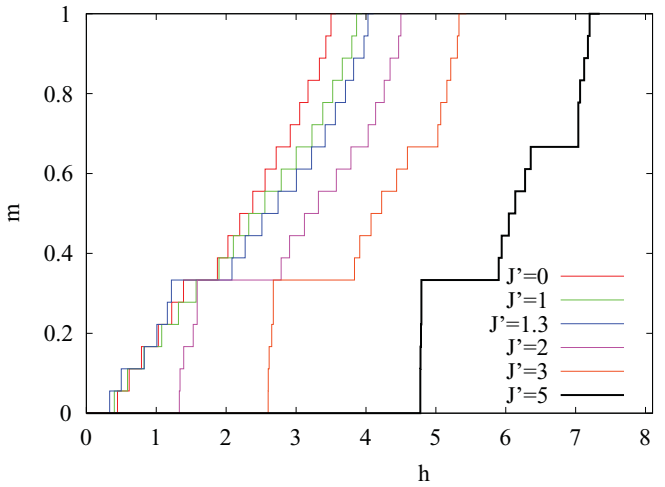

FIG. 8. (Color online) Results for the relative magnetization $m = M/M_{sat}$ vs applied field of strength h obtained via ED for $N = 36$, where M_{sat} is the saturation magnetization.

Altogether, our data for the order parameter, the spin-spin correlation functions, and the pitch angle, lead to the conclusion that there is most likely a direct first-order transition from a magnetically ordered state with spin orientations similar to those of the classical GS to the magnetically disordered orthogonal-dimer singlet GS.

V. MAGNETIZATION PROCESS

The magnetization process of frustrated quantum magnets has attracted much attention due to the discovery of exotic parts of the magnetization curve, such as plateaus and jumps, see, e.g., Refs. 57–61. The magnetization curves for the pure bounce ($J' = 0$) and maple-leaf ($J' = 1$) HAF were discussed already in Ref. 4 based on ED data for $N = 36$, where no indications for plateaus and jumps were found. On the other hand, we have already seen that the interpolating maple-leaf/bounce lattice AF model considered here, for larger values of J', has much in common with the Shastry-Sutherland model, in particular, that both have at zero field an orthogonal-dimer singlet ground state. It is well known that the magnetization curve of the material $SrCu_2(BO_3)_2$ as well as that of the corresponding Shastry-Sutherland model possesses a series of plateaus, see, e.g., Refs. 4 and 62–66. Motivated by this, we study in this section the magnetization curve $M(h)$ (where M is the total magnetization and h is the strength of the external magnetic field) for the interpolating maple-leaf/bounce lattice AF model using ED for $N = 18$ and 36 sites. ED results for the relative magnetization $m = M/M_{sat}$ versus magnetic field h for $N = 36$ sites are shown in Fig. 8. In accordance with previous results,[4] we do not see indications for a plateau for $0 < J' \leqslant 1$. Moreover, it is obvious that the finite-size singlet-triplet gap determining the size of the first plateau at $m = 0$ is small at $J' = 0$, $J' = 1$, and $J' = 1.3$. That corresponds to our finding of a magnetically ordered GS for these values of J', and therefore the $m = 0$ plateau should disappear for $N \to \infty$. However, a finite $m = 0$ plateau exists in that parameter region where the orthogonal-dimer singlet state is the zero-field GS, since this GS is gapped.

As for the Shastry-Sutherland model, there is a well-pronounced 1/3 plateau appearing at larger values of J'. Interestingly, this plateau emerges already for values of J' below $J'_c \approx 1.5$. In Fig. 9, we show the width of the 1/3 plateau versus J' (main panel) as well as the end points of the plateau (inset) for $N = 18$ and 36. We observe a significant change at $J' = J'_{p_{1/3}} \approx 1.07$. Below $J'_{p_{1/3}}$, the typical finite-size behavior appears, i.e., the plateau width shrinks with system size N and it vanishes at $N \to \infty$. By contrast, for $J' > J'_{p_{1/3}}$, there are almost no finite-size effects. The plateau width increases rapidly up to about $J' \approx J'_c$ and then it remains almost constant for $J' \gtrsim J'_c$, where the end points of the plateau grow linearly with J'. Moreover, from Fig. 8, we find that for larger values of $J' \gtrsim 2$, there is a jumplike transition between the $m = 0$ and the $m = 1/3$ plateaus.

As already mentioned above, for the Shastry-Sutherland model a series of plateaus was observed. For the model under

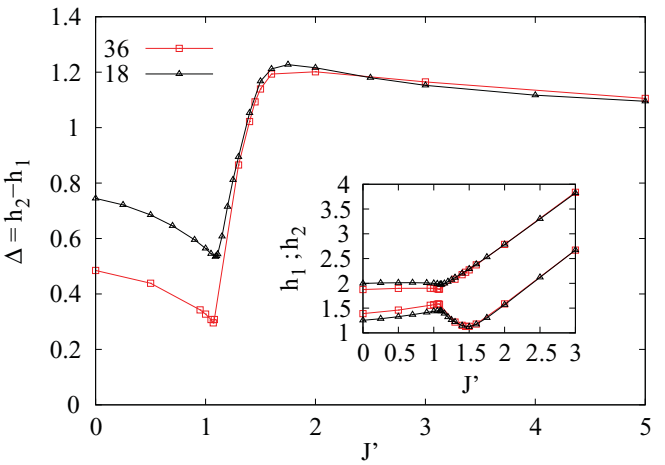

FIG. 9. (Color online) ED results ($N = 18$ and 36) for the $m = 1/3$ plateau. Main panel: width $\Delta = h_2 - h_1$ of the plateau versus J'. Inset: end points h_1 and h_2 of the plateau vs J'.

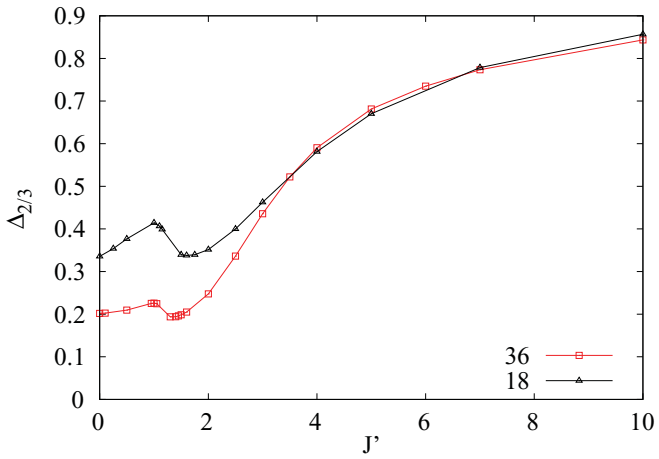

FIG. 10. (Color online) ED results ($N = 18$ and 36) for the width of the $m = 2/3$ plateau in dependence on J'.

consideration here, we find indications for a second plateau at $m = 2/3$, see Figs. 8 and 10. This plateau emerges only for quite large values of $J' > J'_{p_{2/3}} \approx 3$. Again we observe very weak finite-size effects of the plateau width for $J' > J'_{p_{2/3}}$ (see Fig. 10). Furthermore, our ED data suggest an almost direct jump from the $m = 2/3$ plateau to saturation $m = 1$.

Finally, we have to mention that our finite-size analysis of the plateaus naturally could miss other plateaus present in infinite systems, see, e.g., the discussion of the ED data of the $m(h)$ curve of the Shastry-Sutherland model in Ref. 4. Hence, the study of the magnetization process needs further attention based on alternative methods.

VI. CONCLUSIONS

In this paper, we have treated a J-J' spin-half HAF interpolating between the HAF on the maple-leaf ($J' = J$) and the bounce lattice ($J' = 0$). Moreover, we also discuss the GS for larger values $J' > J$. This antiferromagnetic system is geometrically frustrated and it is related to several magnetic materials that have been experimentally investigated recently.[40,41,43] On the classical level, the ground state is a commensurate noncollinear antiferromagnetic state. To study the quantum GS of the spin-half model, we use the CCM for infinite lattices and the ED for finite lattices of $N = 18$ and 36 sites.

We find evidence for a semiclassical magnetically ordered commensurate noncollinear GS in a wide range of the exchange ratio $0 \leqslant J'/J \leqslant J'_c/J \approx 1.45$. However, due to frustration and quantum fluctuations, the sublattice magnetization amounts about 30% of the classical value only. Importantly, we find that at $J'_c \approx 1.45J$ there is a (most likely) first-order transition to a magnetically disordered orthogonal-dimer singlet product GS, which is the exact GS for $J'/J > J'_c/J$, although we cannot rule out that this transition is of second-order type. Therefore the considered model is somewhat similar to the Shastry-Sutherland model. This similarity is also observed in the magnetization curve. Based on ED data we find evidence for plateaus at zero magnetization for $J'/J > J'_c/J$ (which is related to the gapped orthogonal-dimer singlet GS), at $1/3$ of saturation for $J' \gtrsim 1.07J$ and at $2/3$ of saturation for $J' \gtrsim 3J$. The transition to the $1/3$ plateau and from the $2/3$ plateau to saturation can be jumplike. Further plateaus not compatible to the system sizes $N = 18$ and 36, and therefore missed in the ED study, may appear in the infinite system.

This model should be seen in light of a wide range of related 2D quantum spin systems. A very broad spectrum of behavior might occur in these systems, ranging from the case of semiclassical ordering to valence bond solids, spin liquids, and so on. Crucially though, *a priori* one never seems to know what behavior will be seen for a specific 2D model; one needs to simulate the system directly to find out. Indeed, this is what makes these systems so special and interesting. Our results may also stimulate other studies on this interesting 2D frustrated quantum system, using other approximate methods to compare and contrast our results. In particular, the influence of modifications of the exchange bonds, which might be relevant for real-life materials, may lead to a destabilization of magnetic order. Knowing that the corresponding Shastry-Sutherland model exhibits a series of magnetization plateaus, the search for further plateaus may be also an interesting problem to be studied by different means.

ACKNOWLEDGMENTS

For the exact digonalization, J. Schulenburg's SPINPACK was used. The authors are indebted to T. Fennell for providing information on spangolite prior to publication. One of the authors (D.J.J.F.) acknowledges and thanks the European Science Foundation (ESF) for financial support via research network program entitled Highly Frustrated Magnetism (short-visit Grant No. 3858).

[1] E. Manousakis, Rev. Mod. Phys. **63**, 1 (1991).
[2] L. Balents, Nature (London) **464**, 199 (2010).
[3] G. Misguich and C. Lhuillier, in *Frustrated Spin Systems*, edited by H. T. Diep (World Scientific, Singapore, 2004), pp. 229–306.
[4] J. Richter, J. Schulenburg, and A. Honecker, in *Quantum Magnetism*, Lecture Notes in Physics Vol. 645, edited by U. Schollwöck, J. Richter, D. J. J. Farnell, and R. F. Bishop (Springer-Verlag, Berlin, 2004), p. 85.
[5] J. D. Reger, J. A. Riera, and A. P. Young, J. Phys. Condens. Matter **1**, 1855 (1989).
[6] A. Mattsson, P. Fröjdh, and T. Einarsson, Phys. Rev. B **49**, 3997 (1994).
[7] M. Troyer, H. Kontani, and K. Ueda, Phys. Rev. Lett. **76**, 3822 (1996).
[8] L. O. Manuel, M. I. Micheletti, A. E. Trumper, and H. A. Ceccatto, Phys. Rev. B **58**, 8490 (1998).

[9]P. Tomczak and J. Richter, Phys. Rev. B **59**, 107 (1999).
[10]P. W. Anderson, Mater. Res. Bull. **8**, 153 (1973).
[11]P. Fazekas and P. W. Anderson, Philos. Mag. **30**, 423 (1974).
[12]B. Bernu, C. Lhuillier, and L. Pierre, Phys. Rev. Lett. **69**, 2590 (1992).
[13]A. V. Chubukov, S. Sachdev, and T. Senthil, J. Phys. Condens. Matter **6**, 8891 (1994).
[14]L. Capriotti, A. E. Trumper, and S. Sorella, Phys. Rev. Lett. **82**, 3899 (1999).
[15]D. J. J. Farnell, R. F. Bishop, and K. A. Gernoth, Phys. Rev. B **63**, 220402(R) (2001).
[16]D. J. J. Farnell, R. Zinke, J. Schulenburg, and J. Richter, J. Phys. Condens. Matter **21**, 406002 (2009).
[17]B. S. Shastry and B. Sutherland, Physica B **108**, 1069 (1981).
[18]M. Albrecht and F. Mila, Europhys. Lett. **34**, 145 (1996).
[19]E. Müller-Hartmann, R. R. P. Singh, C. Knetter, and G. S. Uhrig, Phys. Rev. Lett. **84**, 1808 (2000).
[20]A. Koga and N. Kawakami, Phys. Rev. Lett. **84**, 4461 (2000).
[21]A. Läuchli, S. Wessel, and M. Sigrist, Phys. Rev. B **66**, 014401 (2002).
[22]R. Darradi, J. Richter, and D. J. J. Farnell, Phys. Rev. B **72**, 104425 (2005).
[23]P. Lecheminant, B. Bernu, C. Lhuillier, L. Pierre, and P. Sindzingre, Phys. Rev. B **56**, 2521 (1997).
[24]Ch. Waldtmann, H. U. Everts, B. Bernu, C. Lhuillier, P. Sindzingre, P. Lecheminant, and L. Pierre, Eur. Phys. J. B **2**, 501 (1998).
[25]D. Schmalfuß, J. Richter, and D. Ihle, Phys. Rev. B **70**, 184412 (2004).
[26]R. R. P. Singh and D. A. Huse, Phys. Rev. B **76**, 180407(R) (2007).
[27]S. Yan, D. A. Huse, and S. R. White, e-print arXiv:1011.6114 (unpublished).
[28]J. Richter, J. Schulenburg, A. Honecker, and D. Schmalfuß, Phys. Rev. B **70**, 174454 (2004).
[29]G. Misguich and P. Sindzingre, J. Phys. Condens. Matter **19**, 145202 (2007).
[30]T.-P. Choy and Y. B. Kim, Phys. Rev. B **80**, 064404 (2009); B.-J. Yang, A. Paramekanti, and Y. B. Kim, *ibid.* **81**, 134418 (2010).
[31]R. Siddharthan and A. Georges, Phys. Rev. B **65**, 014417 (2001).
[32]P. Tomczak and J. Richter, J. Phys. A: Math. Gen. **36**, 5399 (2003).
[33]J. Richter, O. Derzhko, and J. Schulenburg, Phys. Rev. Lett. **93**, 107206 (2004).
[34]J. Richter, J. Schulenburg, P. Tomczak, and D. Schmalfuß, Condens. Matter Phys. **12**, 507 (2009).
[35]D. D. Betts, Proc. N. S. Inst. Sci. **40**, 95 (1995).
[36]D. Schmalfuß, P. Tomczak, J. Schulenburg, and J. Richter, Phys. Rev. B **65**, 224405 (2002).
[37]S. Taniguchi, T. Nishikawa, Y. Yasui, Y. Kobayashi, M. Sato, T. Nishioka, M. Kontani, and K. Sano, J. Phys. Soc. Jpn. **64**, 2758 (1995).
[38]H. Kageyama H. Kageyama, K. Yoshimura, R. Stern, N. V. Mushnikov, K. Onizuka, M. Kato, K. Kosuge, C. P. Slichter, T. Goto, and Y. Ueda, Phys. Rev. Lett. **82**, 3168 (1999).
[39]Y.-Z. Zheng, M.-L. Tong, W. Xue, W.-X. Zhang, X.-M. Chen, F. Grandjean, and G. J. Long, Angew. Chem. Int. Ed. **46**, 6076 (2007).
[40]D. Cave, F. C. Coomer, E. Molinos, H. H. Klauss, and P. T. Wood, Angew. Chem. Int. Ed. **45**, 803 (2006).
[41]T. D. Keene, M.-E. Light, M. B. Hursthouse, and D. J. Price, Dalton Trans. **40**, 2983 (2011).
[42]F. C. Hawthorne, M. Kimata, and R. K. Eby, Am. Mineral. **78**, 649 (1993).
[43]T. Fennell, J. O. Piatek, R. A. Stephenson, G. J. Nilsen, and H. M. Ronnow, J. Phys. Condens. Matter **23**, 164201 (2011).
[44]R. F. Bishop, *Microscopic Quantum Many-Body Theories and Their Applications*, Lecture Notes in Physics Vol. 510, edited by J. Navarro and A. Polls (Berlin, Springer-Verlag, 1998), p. 1.
[45]C. Zeng, D. J. J. Farnell, and R. F. Bishop, J. Stat. Phys. **90**, 327 (1998).
[46]R. F. Bishop, D. J. J. Farnell, S. E. Krüger, J. B. Parkinson, and J. Richter, J. Phys. Condens. Matter **12**, 6877 (2000).
[47]D. J. J. Farnell and R. F. Bishop, in *Quantum Magnetism*, Lecture Notes in Physics Vol. 645, edited by. U. Schollwöck, J. Richter, D. J. J. and R. F. Bishop (Springer-Verlag, Berlin, 2004), p. 307.
[48]J. B. Parkinson and D. J. J. Farnell, in *An Introduction to Lattice Quantum Spin Systems*, Lecture Notes In Physics Vol. 816 (Springer-Verlag, Berlin, Heidelberg, 2010), p. 109–134.
[49]For the numerical calculation, we use the program package "The crystallographic CCM" (D. J. J. Farnell and J. Schulenburg).
[50]Note here that there is a misprint in Ref. 4 concerning the extrapolated GS energy per bond of the maple-leaf lattice. The correct value reads $E_0/\text{bond} = 0.2137$.
[51]G. Misguich, C. Lhuillier, B. Bernu, and C. Waldtmann, Phys. Rev. B **60**, 1064 (1999).
[52]R. F. Bishop, J. B. Parkinson, and Y. Xian, Phys. Rev. B **43**, R13782 (1991); **44**, 9425 (1991).
[53]D. D. Betts and J. Oitmaa, Phys. Lett. A **62**, 277 (1977); J. Oitmaa and D. D. Betts, Can. J. Phys. **56**, 897 (1978).
[54]H. J. Schulz and T. A. L. Ziman, Europhys. Lett. **18**, 355 (1992); H. J. Schulz, T. A. L. Ziman, and D. Poilblanc, J. Phys. I **6**, 675 (1996).
[55]N. Laflorencie and D. Poilblanc, in *Quantum Magnetism*, Lecture Notes in Physics Vol. 645, edited by U. Schollwöck, J. Richter, D. J. J. Farnell, and R. F. Bishop (Springer-Verlag, Berlin, 2004), p. 227.
[56]J. Richter and J. Schulenburg, Eur. Phys. J. B **73**, 117 (2010).
[57]H. Nishimori and S. Miyashita, J. Phys. Soc. Jpn. **55**, 4448 (1986).
[58]A. Honecker, J. Phys. Condens. Matter **11**, 4697 (1999).
[59]C. Lhuillier and G. Misguich, in *High Magnetic Fields*, Lecture Notes in Physics Vol. 595, edited by C. Berthier, L. P. Lévy, and G. Martinez (Springer, Berlin, 2002), p. 161.
[60]J. Schulenburg, A. Honecker, J. Schnack, J. Richter, and H.-J. Schmidt, Phys. Rev. Lett. **88**, 167207 (2002).
[61]A. Honecker, J. Schulenburg, and J. Richter, J. Phys. Condens. Matter **16**, S749 (2004).
[62]H. Kageyama, K. Yoshimura, R. Stern, N. V. Mushnikov, K. Onizuka, M. Kato, K. Kosuge, C. P. Slichter, T. Goto, and Y. Ueda, Phys. Rev. Lett. **82**, 3168 (1999).
[63]K. Kodama, M. Takigawa, M. Horvatic, C. Berthier, H. Kageyama, Y. Ueda, S. Miyahara, F. Becca, and F. Mila, Science **298**, 395 (2002).
[64]G. Misguich, Th. Jolicoeur, and S. M. Girvin, Phys. Rev. Lett. **87**, 097203 (2001).
[65]J. Schulenburg and J. Richter, Phys. Rev. B **65**, 054420 (2002).
[66]J. Dorier, K. P. Schmidt, and F. Mila, Phys. Rev. Lett. **101**, 250402 (2008).
[67]S. E. Sebastian, N. Harrison, P. Sengupta, C. D. Batista, S. Francoual, E. Palm, T. Murphy, N. Marcano, H. A. Dabkowska, and B. D. Gaulin, Proc. Natl. Acad. Sci. USA **107**, 6175 (2010).